XLVI CILAMCE
VITÓRIA - ES - BRAZIL - 2025
XLVI IBERO-LATIN AMERICAN CONGRESS ON COMPUTATIONAL METHODS IN ENGENEERING

Nonlinear vibration analysis of a three-dimensional discrete model for guyed towers with unilateral contact restrictions in the cables

Fernanda Neves da Silva[1], Frederico Martins Alves da Silva[1], Diego Orlando[2]

[1]*School of Civil Engineering, Federal University of Goiás, UFG*
Av. Universitária, n.º 1488 - quadra 86 - Setor Leste Universitário, 74605-010, Goiânia, Goiás, Brasil
fernanda_neves@discente.ufg.br, silvafma@ufg.br
[2]*Department of Mechanical and Energy – FAT, State University of Rio de Janeiro, UERJ*
Av. Dr. Omar Dibo Calixto Afrange, s/n, Access by Rod. Pres. Dutra - km 304, 27537-000, Resende/RJ, Brazil
diego@fat.uerj.br

Abstract. Guyed towers are slender vertical structures anchored by cables (guy wires), widely employed in engineering due to their ability to reach great heights with high structural efficiency. As a result of their slenderness and the interaction between the guy wires and the mast, these towers exhibit complex structural behavior, characterized by pronounced geometric nonlinearities. The cable system provides lateral displacement constraints and is highly efficient when subjected to tensile forces. This study aims to investigate the nonlinear static and dynamic behavior of a guyed tower modeled as a discrete three-dimensional system with two degrees of freedom. A central focus of the analysis is the inclusion of unilateral contact in the guy wires, i.e., the assumption that these elements do not resist compressive forces. This restriction introduces a boundary condition that significantly affects the structural stability, particularly in the post-critical regime. The results demonstrate that the consideration of unilateral contact leads to a significant reduction in the tower's critical load and strongly influences its dynamic behavior. These findings highlight the importance of incorporating geometric nonlinearities and the unilateral behavior of guy wires from the early stages of design to ensure a more realistic and safe structural analysis.

Keywords: Guyed towers, Unilateral constraints, Non-linear static analysis, Nonlinear dynamic analysis.

1 Introduction

Guyed towers are slender vertical structural elements whose lateral stability is ensured by the use of tensioned cables (guys). According to Assis *et al.* [1] and Pasquetti [2], these structures are commonly employed due to their structural efficiency, as they allow for great heights and high load-bearing capacities. Consequently, they are widely used to support telecommunications antennas, transmission lines, wind turbines, offshore platforms, long-span roofs, and bridge decks. One of the main challenges in the design of guyed towers lies in their highly nonlinear behavior, as observed by Marques [3]. This nonlinearity manifests in both the static and dynamic responses of the structure, requiring advanced analytical approaches for an accurate representation of their performance. In this context, Del Prado *et al.* [4] emphasize that geometric nonlinearities have a significant influence on the structural response, especially due to the slenderness and flexibility of these towers. As evidenced by Carvalho [5], the ability of guyed structures to efficiently support axial loads is directly related to the use of cables, which, by acting predominantly in tension, offer excellent structural performance while meeting the architectural and functional requirements of the project.

Despite their structural efficiency, guyed towers exhibit high sensitivity to geometric imperfections and variations in boundary conditions, making stability control a considerable challenge for engineers. Marques [3] and Nielsen [6] report that the highly nonlinear behavior of these structures, particularly due to the action of the cables, is directly associated with partial or total collapses that have been observed in practice. Barbosa [7] notes that certain structures are subject to unilateral contact conditions, in which resistance to displacement exists only

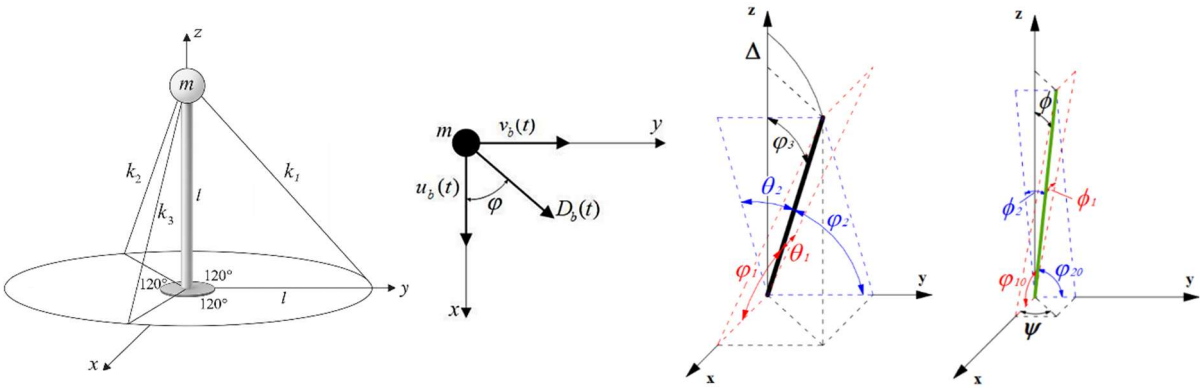
in specific directions. In this regard, guyed towers represent a class of structures for which this type of contact must be considered, since cables only exert force when under tension. Therefore, including the hypothesis of unilateral contact in the modeling of cable behavior is essential for constructing more accurate and representative mathematical models of structural stability.

Thus, the present work aims to investigate the effects of unilateral contact on the nonlinear static and dynamic behavior of guyed towers. The presence of this contact condition alters the internal force distribution and the equilibrium conditions of the structure, requiring a formulation that adequately accounts for the constraints imposed by the cables in order to ensure a realistic structural behavior model.

2 Mathematical formulation

The simplified three-dimensional model adopted in this research is based on the formulation presented by Orlando [8], which, in turn, is grounded in the classical studies of Thompson and collaborators (Thompson and Gaspar [9]; Thompson and Hunt [10]; Thompson and Stewart [11]), widely recognized in the analysis of the nonlinear behavior of guyed towers. The guyed tower, given by Fig. 1(a), consists of a central rigid rod of length l, pinned at the lower end and free at the upper end, where a vertical axial load corresponding to the weight of a concentrated mass m is applied. Lateral displacements are restrained by three inclined linear springs, representing the guy wires. The spring with stiffness k_1 lies in the yz-plane, while springs k_2 and k_3 are symmetrically arranged with respect to the y-axis, forming an angle of 120° with this axis, as illustrated in Fig. 1(a). These elements simulate the action of guys in different directions of the three-dimensional space. In addition, the system is subjected to a harmonic base excitation, represented by $D_b(t)$. This force is decomposed into two components, $u_b(t)$ in the x-direction and $v_b(t)$ in the y-direction, as illustrated in Fig. 1(b).

The spatial configuration of the rod is described by the angles θ_1 and θ_2, which correspond to the complements of the direction cosines of the rod's orientation, and by the vertical displacement Δ of its top. Also, the angles φ_1, φ_2, and φ_3 define the initial geometric imperfection of the column with respect to the x, y and z-axes, respectively, as illustrated in Fig. 1(c). The problem formulation also considers the influence of the relative stiffness of the springs and the presence of geometric imperfections, represented by the angles $\emptyset_1$ and $\emptyset_2$, associated respectively with the degrees of freedom θ_1 and θ_2, respectively, as shown in Fig. 1(d). These angles describe the initial tilt of the rod with respect to the vertical and serve as parameters to simulate initial imperfections that affect the equilibrium configuration of the system.



(a) (b) (c) (d)

Figure 1. (a) Guyed mast model, (b) Base excitation [12], (c) Perfect deformed system [12], and (d) Geometrically imperfect deformed system [12].

The study of stability based on the energy criterion relates the internal strain energy to the work performed by the external forces acting on the structure. Considering that each spring behaves as a linearly elastic element with stiffness k_i and elongation ΔL_i, the expression for the total elastic energy is given by:

$$U = \frac{1}{2}\, k_1\, \Delta L_1^2 + \frac{1}{2}\, k_2\, \Delta L_2^2 + \frac{1}{2}\, k_3\, \Delta L_3^2. \tag{1}$$

The gravitational potential refers to the work performed by the gravitational force acting on the concentrated mass *m*, and is expressed as:

$$W = P\, \Delta_f\,, \tag{2}$$

where Δ_f corresponds to the difference between the total vertical displacement Δ, observed at the free end of the rod, and the displacement Δ_0, associated solely with the initial geometric imperfections of the structure. Thus, the gravitational potential is expressed as:

$$W = P(\Delta - \Delta_0). \tag{3}$$

To simplify the formulation, the auxiliary variables $u_1 = sen\,\theta_1$ and $u_2 = sen\,\theta_2$ are introduced and used as the two degrees of freedom of the system [8]. The variations in the lengths of the springs, ΔL_1, ΔL_2 e ΔL_3, as well as the vertical displacement of the mass *m*, Δ_f, are given by:

$$\begin{aligned}
\Delta L_1 &= l\sqrt{2 - 2\,sin(\emptyset_2)} - l\sqrt{2 - u_2} \\
\Delta L_2 &= l\sqrt{(sin(\beta) - sin(\emptyset_1))^2 + (cos(\beta) - sin(\emptyset_2))^2 + 1 - sin(\emptyset_1)^2 - sin(\emptyset_2)^2} \\
&\quad - l\sqrt{\sqrt{(sin(\beta) - u_1)^2 + (cos(\beta) - u_2)^2 + 1 - {u_1}^2 - {u_2}^2}}, \\
\Delta L_3 &= l\sqrt{(-sin(\beta) - sin(\emptyset_1))^2 + (cos(\beta) - sin(\emptyset_2))^2 + 1 - sin(\emptyset_1)^2 - sin(\emptyset_2)^2} \\
&\quad - l\sqrt{\sqrt{(-sin(\beta) - u_1)^2 + (cos(\beta) - u_2)^2 + 1 - {u_1}^2 - {u_2}^2}} \\
\Delta_f &= l\,(\sqrt{1 - {u_1}^2 - {u_2}^2} - \sqrt{1 - \sin(\emptyset_1)^2 - \sin(\emptyset_2)^2})
\end{aligned} \tag{4}$$

In this work $\beta = 120°$, see Fig. 1(a).

Thus, the total potential energy of the system, $\Delta\pi = U - W$, is given by:

$$\Delta\pi = \frac{1}{2}\sum_{i=1}^{3} FS_i\, k_i\, (\Delta L_i)^2 - P\, l\,(\sqrt{1 - {u_1}^2 - {u_2}^2} - \sqrt{1 - sin(\emptyset_1)^2 - sin(\emptyset_2)^2}), \tag{5}$$

where the parameter FS_i represents the *Signum* function, which introduces the consideration of unilateral contact into the formulation. This mathematical function extracts the sign of a real (or complex) number and, when applied to the internal strain energy terms associated with the cables, serves the purpose of excluding those elements subjected to compression. In this context, to properly account for unilateral contact behavior, FS_i must assume the following expressions:

$$FS_1 = \left(\frac{signum(\Delta L_1)}{2} + \frac{1}{2}\right), FS_2 = \left(\frac{signum(\Delta L_2)}{2} + \frac{1}{2}\right), FS_3 = \left(\frac{signum(\Delta L_3)}{2} + \frac{1}{2}\right) \tag{6}$$

However, for an analysis that does not consider the constraint imposed by unilateral contact - i.e., when the effects of all cables are included in the study of the structural system behavior (bilateral contact) - FS_i must assume a unitary value.

As adopted by Thompson and Gaspar [9], it is assumed that the stiffnesses of springs k_2 and k_3 are equal, given by $k_2 = k_3 = v\,K$, where v is a positive constant. The stiffness of spring k_1, in turn, is defined as:

$$k_1 = (1 - 2\,v)\,K, \tag{7}$$

The dimensionless potential energy is therefore given by:

$$\overline{\Delta\pi} = \frac{\Delta\pi}{ml^2} = \sum_{i=1}^{3} FS_i\, \frac{2\omega_p^2}{3\lambda}\, (\Delta L_i)^2 - \omega_p^2\, \left(-\sqrt{1 - {u_1}^2 - {u_2}^2} + \sqrt{1 - sin(\emptyset_1)^2 - sin(\emptyset_2)^2}\right). \tag{8}$$

The equations are nondimensionalized with respect to the critical load of the perfect system, $P_{cr} = Kl/4$. Additionally, the following auxiliary variables are adopted: $P = mg$, $v = \alpha/4\,\sin\beta^2$, $\omega_p^2 = g/l$, $K/m\,l^2 = \omega_p^2/\lambda$, $\alpha = k_1 / k_2$ and $\lambda = P/P_{cr}$.

The kinetic energy is expressed as:

$$\bar{T} = \frac{T}{ml^2} = \frac{1}{2}\left((\dot{u}_1 + \dot{u}_b)^2 + (\dot{u}_2 + \dot{v}_b)^2 - \frac{(u_1\dot{u}_2 + u_2\dot{u}_2)^2}{{u_1}^2 + {u_2}^2 - 1}\right) \tag{9}$$

The equations of motion of the system are derived based on Hamilton's principle, which governs the temporal evolution of the variables u_1 and u_2, expressed by the differential equations that describe the system's dynamics:

$$\frac{\mathrm{d}}{\mathrm{d}t}\frac{\partial \bar{T}}{\partial \dot{u}_i} - \frac{\partial \bar{T}}{\partial u_i} + \frac{\partial \bar{V}}{\partial u_i} = 0 \tag{10}$$

Based on eq. (10), the equations of motion of the system are obtained in terms of the generalized coordinates u_1 and u_2, as presented below:

$$\begin{aligned}
&\ddot{u}_1(1 - u_1^2 - 2u_2^2 + u_1^2u_2^2 + u_2^4) + \ddot{u}_2(u_1u_2 - u_1^3u_2 - u_1u_2^3) + \dot{u}_1^2\,(u_1 - u_1u_2^2) + \dot{u}_2^2\,(u_1 - u_1^3) \\
&\quad + 2u_1^2u_2\dot{u}_1\dot{u}_2 \\
&\quad + \left\{\frac{2}{\sqrt{3}\lambda\,\Omega^2}\left[-FS_2\left(\frac{\sqrt{2-\sqrt{3}\,u_{10}+u_{20}} - \sqrt{2-\sqrt{3}\,u_1+u_2}}{\sqrt{2-\sqrt{3}u_1+u_2}}\right)\right.\right. \\
&\quad \left.\left. - FS_3\left(\frac{\sqrt{2+\sqrt{3}\,u_{10}+u_{20}} - \sqrt{2-\sqrt{3}\,u_1+u_2}}{\sqrt{2+\sqrt{3}u_1+u_2}}\right)\right] - \frac{1}{\Omega^2}\frac{u_1}{\sqrt{1-u_1^2-u_2^2}}\right. \\
&\quad \left. + \frac{2\xi\dot{u}_1}{\Omega}\right\}({u_1}^2 + {u_2}^2 - 1)^2 = F\cos(\varphi)\sin(\tau)\;({u_1}^2 + {u_2}^2 - 1)^2
\end{aligned} \tag{11}$$

$$\begin{aligned}
&\ddot{u}_2(1 - u_2^2 - 2u_1^2 + u_1^2u_2^2 + u_1^4) + \ddot{u}_1(u_1u_2 - u_1^3u_2 - u_1u_2^3) + \dot{u}_2^2\,(u_2 - u_2u_1^2) \\
&\quad + \dot{u}_1^2\,(u_2 - u_2^3)\,2u_1^2u_2\dot{u}_1\dot{u}_2 \\
&\quad + \left\{-\frac{2}{\sqrt{3}\lambda\,\Omega^2}\left[FS_2\left(\frac{\sqrt{2-\sqrt{3}\,u_{10}+u_{20}} - \sqrt{2-\sqrt{3}\,u_1+u_2}}{\sqrt{2-\sqrt{3}u_1+u_2}}\right)\right.\right. \\
&\quad \left.\left. - FS_3\left(\frac{\sqrt{2+\sqrt{3}\,u_{10}+u_{20}} - \sqrt{2-\sqrt{3}\,u_1+u_2}}{\sqrt{2+\sqrt{3}u_1+u_2}}\right)\right]\right. \\
&\quad \left. + FS_1\left(\frac{4\sqrt{2-2u_{20}} - 4\sqrt{2-2u_2}}{3\lambda\Omega^2\sqrt{2-2u_2}}\right) - \frac{1}{\Omega^2}\frac{u_2}{\sqrt{1-u_1^2-u_2^2}} + \frac{2\xi\dot{u}_2}{\Omega}\right\}({u_1}^2 + {u_2}^2 \\
&\quad - 1)^2 = F\cos(\varphi)\sin(\tau)\,({u_1}^2 + {u_2}^2 - 1)^2,
\end{aligned} \tag{12}$$

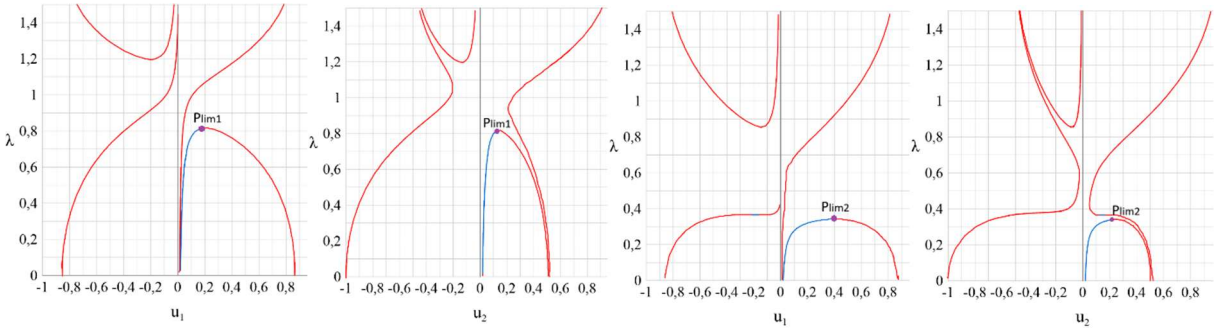
where ξ is the damping coefficient, and $u_{10} = sin(\emptyset_1)$, $u_{20} = sin(\emptyset_2)$, $\tau = \omega_e t$, $F = D_b\,/\,l$, $\Omega = \omega_e\,/\,\omega_p$, $C_i/ml^2 = 2\xi/\Omega$.

3 Numerical results

Initially, a nonlinear static analysis is conducted. For that, the following parameter values were adopted: $\alpha = 1, \omega_p = 1, \emptyset_1 = 1°$ and $\emptyset_2 = 1°$. Figures 2(a) and 2(b) presents the nonlinear equilibrium paths of the structural system considering bilateral contact while Fig. 2(c) and 2(d) displays the influence of unilateral contact on these equilibrium paths. The nonlinear equilibrium paths are represented in the orthogonal planes $\lambda \times u_1$ and $\lambda \times u_2$, and the curves plotted in blue indicate stable equilibrium configurations while the plotted red lines represent unstable segments of the nonlinear static response.

From these figures, it is observed, when analyzing the mast rotations ranging from 0 to 1, that the existing

solutions differ when comparing the two types of cable contact. The presence of an initial imperfection in the mast causes an initial displacement of the structure. Therefore, no bifurcation point is observed, and the left and right branches of the nonlinear equilibrium path are no longer symmetric under these conditions.



(a) (b) (c) (d)

Figure 2. Post-critical path of the model that considers (a) bilateral contact in the $\lambda \times u_1$ plane, (b) bilateral contact in the $\lambda \times u_2$ plane, (c) unilateral contact in the $\lambda \times u_1$ plane, (d) unilateral contact in the $\lambda \times u_2$ plane.

In the absence of a critical load, the analysis focuses on the limit load, associated with small displacements and belonging to stable trajectories. In both cases, as common behavior, when the axial compressive load increases, a stable nonlinear path emerges, with an increase in effective stiffness up to a certain maximum limit point, P_{lim}. However, it is important to note that the limit load for the unilateral contact case is lower than the one obtained under bilateral contact conditions ($P_{lim2} < P_{lim1}$). The significant loss of stiffness in the structural system when unilateral contact constraints are considered is evidenced by comparing the post-critical paths of Fig. 2.

Furthermore, when comparing the trajectories for the two types of contact, it is noted that the stable branches do not coincide precisely within the same range of rotations. However, the system exhibits larger stability intervals when unilateral contact is considered. This comparison highlights that unilateral contact acts as a stabilizing factor in certain regions of the post-critical path, while also introducing greater asymmetry in the equilibrium trajectories of the system.

Now, the dynamic analysis is carried out to investigate the vibratory behavior of the guyed tower subjected to harmonic base excitation, considering the unilateral contact of the cables. For this analysis, the following parameter values are adopted: $\lambda = 0.1, F = 0.01, \varphi = 0$ and $\xi = 0.05$. Figure 4(a) shows the resonance curves in the $u_{1\,max}$ x Ω plane for a guyed tower with the initial imperfections $\emptyset_1 = \emptyset_2 = 1^{\circ}$. These imperfection angles cause the guyed tower to have two compressed cables and only one under tension, as illustrated in Fig. 3(a). Consequently, due to unilateral contact conditions, the tower's initial configuration relies on a single cable for stabilization. in this configuration. The resonance curves are obtained using the *MatCont* package numerical routines, which enables the numerical continuation of periodic solutions and the automatic detection of bifurcations [13].

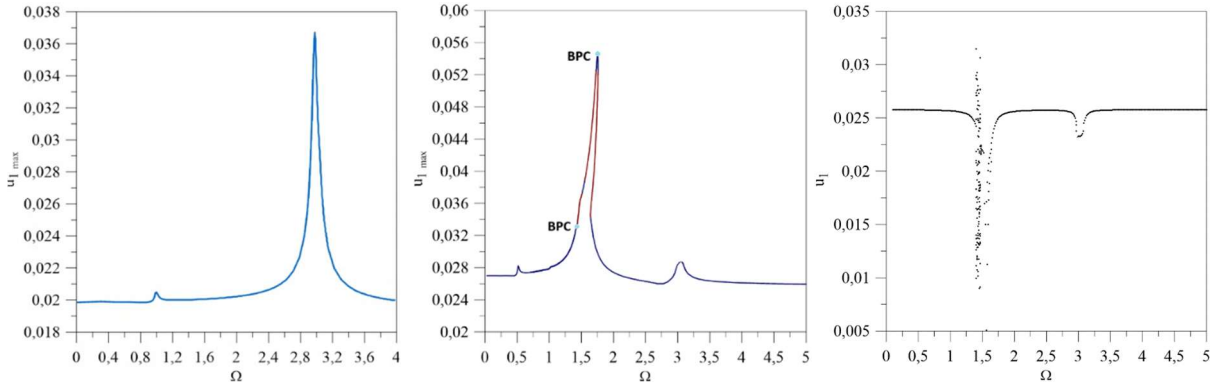


(a) (b)

Figure 3. Cable configuration for two distinct geometric imperfection conditions of the mast: (a) $\emptyset_1 = \emptyset_2 = 1^{\circ}$ and (b) $\emptyset_1 = \emptyset_2 = -1^{\circ}$. Red element is related to compression. Blue element is related to tension.

Figure 4(a) presents the resonance curve obtained for the imperfect bilateral contact model with $\emptyset_1 = \emptyset_2 = 1^{\circ}$, where the system exhibits small vibration amplitudes outside the resonance regions, remaining entirely on

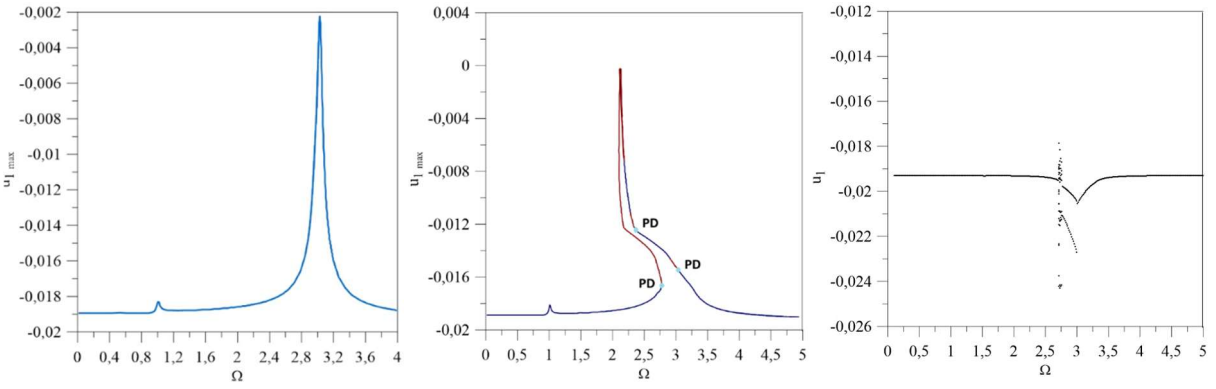
stable trajectories (shown in blue). In contrast, Fig. 4(b), which refers to the imperfect unilateral contact model, reveals a significantly different behavior, with an abrupt increase in amplitude as the excitation frequency approaches the primary resonance region ($\Omega \approx 1.5$), followed by a discontinuity and the emergence of an unstable branch (in red), typical of systems undergoing saddle-node bifurcations (BPC). Figure 4(c) displays the Poincaré sections of the unilateral contact model at different excitation frequencies, where well-defined points appear in the stable regions, while scattered cloud-like patterns are observed near the unstable branch, indicating chaotic behavior and loss of periodicity. These differences highlight the significant impact of unilateral contact on the dynamic stability of the system.



(a) (b) (c)

Figure 4. (a) Resonance curve — bilateral contact, $\emptyset_1 = \emptyset_2 = 1^\circ$, (b) Resonance curve — unilateral contact, $\emptyset_1 = \emptyset_2 = 1^\circ$and (c) Poincaré sections for unilateral contact.

An initial geometric imperfection $\emptyset_1 = \emptyset_2 = -1^\circ$ is now considered. This configuration is illustrated in Fig. 3(b), which shows that the resulting geometry has one compressed cable and two tensioned cables. For this case, the resonance curves for bilateral and unilateral contact hypotheses of the cables and Poincaré mapping are presented in Figs. 5(a), 5(b), and 5(c), respectively. Figure 5(a) corresponds to the imperfect bilateral contact model, where all solutions remain stable throughout the entire excitation frequency range. In contrast, Fig. 5(b) presents the response of the unilateral contact model, in which a peak is observed around the excitation frequency $\Omega \approx 3.0$, followed by the emergence of an unstable branch highlighted in red. It is important to note that the initial geometric imperfection increases the number of tensioned cables, which in turn raises the natural frequency and shifts the resonance peak. As in the previous case, the periodic solution is valid only in part of the excitation interval. The instability is confirmed by the Poincaré sections shown in Fig. 5(c), where scattered point clouds indicate a loss of periodicity and the presence of chaotic behavior. In this case, a period-doubling (PD) bifurcation is also observed, marking the transition to more complex dynamics.



5

(a) (b) (c)

Figure 5. (a) Resonance curve — bilateral contact, $\emptyset_1 = \emptyset_2 = -1^\circ$, (b) Resonance curve — unilateral contact, $\emptyset_1 = \emptyset_2 = -1^\circ$and (c) Poincaré sections for unilateral contact.

The introduction of geometric imperfections directly influences the initial state of tension or compression in the guy wires, as illustrated in Fig. 3. When there is an initial tilt of the mast, $\emptyset_1 = 1^\circ$ and $\emptyset_2 = 1^\circ$ (see Fig. 3(a)), only one cable remains in tension (in blue), while the other cables tend to be compressed, indicating that they are disregarded under unilateral contact conditions. Conversely, in the configuration with $\emptyset_1 = -1^\circ$ and $\emptyset_2 = -1^\circ$ (see Fig. 3(b)) two cables are under tension. This asymmetry introduced by the imperfection and reinforced by the unilateral contact condition significantly affects the system's stiffness, the post-critical equilibrium paths, and the nonlinear dynamics of the structure, including a direct impact on the stability limits and the occurrence of bifurcations.

4 Conclusions

This work presented a nonlinear static and dynamic analysis of a three-dimensional discrete model for guyed towers, considering the presence of unilateral contact constraints in the cables and geometric imperfections in the mast. The results showed that unilateral behavior significantly alters the internal force distribution by eliminating the contribution of cables under compression and introducing strong asymmetries in the post-critical response. Compared to the bilateral contact model, the unilateral formulation resulted in a reduction of the limit load and modifications in the stability range. From a dynamic perspective, the system exhibited regions of instability and aperiodic behavior near resonance, as evidenced by bifurcations in the response curves and by the Poincaré sections. These findings highlight the importance of adopting more realistic models capable of reflecting the actual physical behavior of guyed towers subjected to large displacements and directional constraints.

Acknowledgements. This work was supported by the Brazilian research agencies: CNPq, CAPES, FAPEG.

Authorship statement. The authors hereby confirm that they are the sole liable persons responsible for the authorship of this work, and that all material that has been herein included as part of the present paper is either the property (and authorship) of the authors, or has the permission of the owners to be included here.

References

[1] M. F. de Assis *et al.*, *Vibrações não lineares e estabilidade de torres estaiadas*. Undergraduate thesis, Instituto Federal de Educação, Ciência e Tecnologia de Goiás, 2018.
[2] E. Pasquetti. *Estabilidade Estática e Dinâmica de Torres Estaiadas.* Master's thesis, Pontifícia Universidade Católica do Rio de Janeiro (PUC-Rio), 2003.
[3] I. R. Marques. *Influence of Nonlinear Normal Modes and Symmetries on the Dynamic of a Slender Guyed Tower*. Master's thesis, Pontifícia Universidade Católica do Rio de Janeiro (PUC-Rio), 2020.
[4] Z. J. Del Prado, E. C. Carvalho and P. B. Gonçalves, "Dynamic stability of imperfect cable stayed masts". *Mecánica Computacional*, vol. 29, n. 7, pp. 647-658, 2010.
[5] E. C. Carvalho. *Análise da Instabilidade Dinâmica de Estruturas Estaiadas*. *Master's thesis*, Universidade Federal de Goiás, 2008.
[6] M. G. Nielsen. *Guyed Masts Exposed to Guy Failure*. In: *Structures Congress 2006: Structural Engineering and Public Safety*, St. Louis, Missouri, USA. Proceedings: *Structural Engineering and Public Safety*, pp. 1–10, 2006.
[7] H. J. C. Barbosa. *Algoritmos numéricos para problemas de contato em elasticidade*. PhD thesis, Universidade Federal do Rio de Janeiro, Rio de Janeiro, 1986.
[8] D. Orlando. *Dinâmica Não-Linear, Instabilidade e Controle de Sistemas Estruturais com Interação Modal*. Phd thesis, Pontifícia Universidade Católica do Rio de Janeiro (PUC-Rio), 2010.
[9] J. M. T. Thompson and Z. Gaspar. "A Buckling Model for the Set of Umbilic Catastrophes". *Mathematical Proceedings of the Cambridge Philosophical Society*, vol. 82, p. 497-507, 1977.
[10] J. M. T. Thompson and G. W. Hunt. *Elastic Instability Phenomena*. John Wiley & Sons, London, 1984.
[11] J. M. T. Thompson and H. B. Stewart. *Nonlinear Dynamics and Chaos*. John Wiley & Sons, Chichester, 1987.
[12] D. Orlando, P. B. Gonçalves, S. Lenci and G. Rega, "Nonlinear dynamics and sensitivity to imperfections in guyed mast". *Journal of Vibration Testing and System Dynamics*, vol. 9, n. 2, pp. 109-121, 2025.
[13] A. Dhooge, W. Govaerts and Y. A. Kuznetsov. "MATCONT: A MATLAB package for numerical bifurcation analysis of ODEs". ACM *Transactions on Mathematical Software*, vol. 29, n. 2, pp. 141–164, 2003.